Atmos. Meas. Tech. Discuss., 4, 5773–5806, 2011
www.atmos-meas-tech-discuss.net/4/5773/2011/
doi:10.5194/amtd-4-5773-2011

Atmospheric Measurement Techniques Discussions

Sensitivity study on polarized aerosol retrievals of PARASOL in Beijing and Kanpur

X. F. Gu[1,3], S. P. Wang[1,2,3], L. Fang[1,2,3], T. Yu[1,3], and J. Gao[4]

[1]State Key Laboratory of Remote Sensing Science, Jointly Sponsored by the Institute of Remote Sensing Applications of Chinese Academy of Sciences and Beijing Normal University, Beijing, China
[2]Graduate University of Chinese Academy of Sciences, Beijing, China
[3]The Center for National Spaceborne Demonstration, Beijing, China
[4]Administration on Science, Technology, and Industry for National Defense, Beijing, China

Received: 9 July 2011 – Accepted: 5 September 2011 – Published: 12 September 2011

Correspondence to: S. P. Wang (wangsp@irsa.ac.cn)

Published by Copernicus Publications on behalf of the European Geosciences Union.

Abstract

Sensitivity study on the PARASOL aerosol retrieval algorithm over land is presented for aerosol mixtures composed of fine mode pollution particles combined with coarse mode desert dust. First an assessment of the PARASOL aerosol products during the period of 2005–2009 is investigated by comparison with AOD derived by AERONET (Aerosol Robotic Network) at Beijing and Kanpur.

Validation against AERONET fine mode AOD shows an overall high correlation of $R^2 = 0.79$ for Beijing and $R^2 = 0.83$ for Kanpur. However, the PARASOL retrievals are found to underestimate aerosol optical depth by about 27 % and 34 % for Beijing and Kanpur, respectively. The AOD agreement is obviously poorer as compared to AERONET total AOD, showing underestimation by 60 % and 67 %. At both sites, the PARASOL retrieval algorithm performs better in autumn and winter seasons with the best appearing in autumn.

As PARASOL aerosol algorithm is sensitive to the accumulation mode of the aerosol size distribution, we conduct study on the threshold radius of this fraction of size distribution, named as sensitive radius, for different seasons at both Beijing and Kanpur. The results show that the sensitive radius for polarized aerosol retrieval is 0.35 µm for all seasons. And the agreement is significantly improved by employing comparison against the AERONET AOD recomputed for radius <0.35 µm, showing a correlation coefficient (R^2) of 0.82 with relative difference being 12 % for Beijing and 0.87 with relative difference being 19 % for Kanpur.

The sensitivity study on uncertainty of PARASOL aerosol retrieval demonstrates that uncertainties caused by the algorithm-assumed refractive index and size distribution are significantly higher in spring than those of autumn and winter seasons. The aerosol retrieval errors caused by aerosol polarized phase function $q_a(\Theta)$ for spring are found to be higher at Kanpur, due to the obviously higher content of coarse dust particles.

For all seasons the aerosol retrieval errors contributed by uncertainty in $q_a(\Theta)$ are much close to the total retrieval errors (accounts for about 65 % to 94 % in different

seasons), indicating that the overestimate of $q_a(\Theta)$ in PARASOL algorithm accounts for most of the underestimate of retrieved AOD at both sites.

Investigation on the uncertainty of surface contribution shows that the surface model overestimates surface polarization from about 20 % to 50 % with the maximum uncertainties occurring in winter.

1 Introduction

Radiative forcing of global climate change by tropospheric aerosols is thought to contribute substantially to the radiative balance of the Earth-atmosphere system. Both the direct scattering of shortwave solar radiation and the enhancement on brightness of clouds caused by increased concentration of cloud condensation nuclei are identified to exert a cooling influence on the planet (Nemesure et al., 1995; Hansen et al., 1997). The anthropogenic aerosols such as biomass burning smoke and urban industrial pollution, typically fine mode particles with radius of roughly 0.1–0.2 µm, are identified to be strong absorbing and have imposed a substantially perturbation to radiative forcing of climate with importance comparable to that of greenhouse gases. (Charlson et al., 1992; Ramanathan et al., 2001). However, the anthropogenic aerosol radiative influence represents a larger uncertainty in climate change research than forcing by greenhouse gases (Hansen et al., 2005). Better estimates of the perturbations to earth's radiation budget require accurate optical and physical properties of fine aerosols such as spectral aerosol optical depth (AOD, ±0.02), size distribution (effective radius ±10 %, effective variance ±40 %) and single scattering albedo (SSA, ±0.03) (Mishchenko et al., 2007). Daily determination of these parameters on a global scale can be achieved by satellite remote sensing (Kaufman et al., 1997; Levy et al., 2007; Deuzé et al., 2001; Martonchik et al., 1998; Kahn et al., 2010; Kokhanovsky and Leeuw, 2009).

Multi-directional and polarized measurements provide more robust aerosol retrievals over land because the reflectance from the surface shows little polarization while that of fine aerosol is highly polarized (Herman et al., 1997b; Deuzé et al., 1999). As a

AMTD
4, 5773–5806, 2011

consequence, the polarized satellite radiances are more sensitive to the presence of aerosols than the total radiances. On the other hand, coarse aerosols, such as desert dust, almost do not polarize sunlight so that the aerosol retrieval using polarized light focuses on small spherical particles like anthropogenic pollutions and biomass burning aerosols. PARASOL (Polarization and Anisotropy of Reflectances for Atmospheric Science coupled with Observations from a Lidar) is the only currently operating satellite that performs multidirectional and polarized measurements. Descriptions of PARASOL mission and the instrument are detailed in Deschamps et al. (1994) and Tanré et al. (2011). The aerosol retrieval algorithm proposed by Deuzé et al. (2001) is based on polarized measurements at 670 and 865 nm. A brief introduction on the algorithm is given in Sect. 2.

A new aerosol retrieval algorithm developed by Dubovik et al. (2011) is an attempt to enhance aerosol retrieval by emphasizing statistical optimization using the data redundancy available from advanced satellite observations (Dubovik et al., 2004, 2011). Based on this strategy, the algorithm aims at retrieval of an extended set of aerosol parameters including the particle size distribution, complex refractive index, parameters characterizing aerosol particle shape and vertical distribution. Also, the approach allows the retrieval of both the optical properties of aerosol and underlying surface over land. The retrieved values of AOD agree reasonably well with AERONET data with correlation coefficient of ~0.9 for Banizoumbou (Niger) and ~0.87 for Mongu (Zambia) (Dubovik et al., 2011). At large aerosol loading with AOD (0.44 µm) >1.0, the approach tends to produce a slight overestimation of the AOD, which is due to the fact that the current algorithm cannot distinguish cases with no absorption and weak absorption of radiation by aerosol particles (Kokhanovsky et al., 2010). Compared with the PARASOL standard algorithm, the new algorithm provides more parameters of aerosols and surface reflectance with better robustness. But the computation and time consumption are increased. As most aerosol pollutions are anthropogenic fine particles, aerosol properties retrieved by Deuzé et al. (2001) can meet the need for evaluating the effects of human activities on climate change. Since both algorithms require prior assumptions on aerosol properties and surface reflectance, sensitivity study on the influence factors of polarized aerosol retrieval is meaningful for improvement in retrieval accuracy and convergence speed.

The two urban AERONET sites chosen in this paper (see in Fig. 1), Beijing, China and Kanpur, India, are located in Asian monsoon regions and both suffer from air pollution of fine anthropogenic aerosols and coarse desert dust. As the capital of China, Beijing (39.9° N, 116.4° E) is a mega-city with a population of approximately 22 million (based on statistics from 2010). It is located along the northwestern border of the Great Plain of North China. Kanpur (26.4° N, 80.3° E) is an important industrial city in northern India with approximately 5 million inhabitants and is located along the southern flank of the central part of the Indo-Gangetic basin. AERONET measurements collected at both sites show high aerosol loading with monthly average mean AOD (0.5 µm) >0.4 throughout the year (Eck et al., 2010). Also, both locations have similar aerosol types characterized as bimodal size distributions (Yu et al., 2009; Singh et al., 2004).

The current study is devoted to examination on the sensitivity of PARASOL aerosol retrievals to both aerosol and surface properties, to improve understanding of the properties required to reduce the uncertainty in retrieved AOD. Section 2 presents the AERONET instrumentation and methodology and the PARASOL aerosol retrieval algorithm, as well as description on how the AOD coincidences were selected. Section 3 summarizes the algorithm performance from the validation dataset during the period of 2005–2009 at Beijing and Kanpur AETONET sites; Sect. 4 looks in detail at the sensitivity of PARASOL aerosol retrieval to aerosol and surface properties. Finally, conclusions are presented in the last section.

2 Data description and methods

2.1 AERONET data

The AERONET is a ground-based aerosol network consisting of more than 400 permanent and temporary sites worldwide (Holben et al., 1998, 2001). The CIMEL Electronique CE-318 Sun and sky radiometer used at AERONET sites operates in two modes: (1) one mode where direct Sun measurements are made every 15 min at 340, 380, 440, 500, 675, 870, 940, and 1020 nm (nominal wavelengths) to compute AOD and CWV and (2) a second mode where sky measurements at 440, 675, 870, and 1020 nm are made in order to retrieve column-integrated microphysical and optical properties (Holben et al., 1998, 2001). Aerosol parameters are retrieved from measured radiances at suitable wavelengths using a radiative transfer model for spherical, non-spherical and mixed types of particles (Dubovik and King, 2000; Dubovik et al., 2006). The aerosol volume size distribution is retrieved in the particle radius range of 0.05–15 µm. The uncertainty in computed AOD, due primarily to the calibration uncertainty, is 0.01–0.02, whereas for optical properties, it is $< \pm 5\,\%$. However, the uncertainty increases for low aerosol loading (Dubovik et al., 2000). To ensure sufficient sensitivity to aerosol absorption, only sky measurements where AOD (440 nm) >0.4 were utilized for the investigation of the characteristics of spectral refractive indices and SSA. In the AERONET database, three levels of data are distributed: Level 1.0 (unscreened with possible cloud contamination), Level 1.5 (cloud screened following the methodology of Smirnov et al., 2000) and Level 2.0 (quality assured with post-deployment calibrations).

For assessment of PARASOL derived AOD at 865 nm, the coincident measurements and fine mode AOD at 870 nm retrieved by AERONET are considered for comparison. As the Level 2.0 retrievals close to satellite overpass time were generally not available, Level 1.5 retrievals are used to ensure enough match-ups for comparison. Moreover, to keep the stable atmospheric conditions for comparing satellite and ground-based

AMTD
4, 5773–5806, 2011

data, the closest AERONET retrievals within half an hour of satellite overpass time are selected in this work.

2.2 PARASOL Level 2 aerosol products

The current standard aerosol inversion strategy, detailed in Deuzé et al. (2001), is based on the LUT (Look-Up Tables) approach, where the reflected radiances are simulated for 10 aerosol models (log-normal size distributions) with effective radius from 0.075 to 0.225 µm and a mean refractive index m = 1.47–0.01i. The aerosol parameters are adjusted to give the best agreement between the measured and simulated multi-directional polarized radiances at 0.67 and 0.865 µm. The contribution from the surface to the polarized reflectance is based on a priori values (as a function of observation geometry and surface type) derived from a statistical analysis of POLDER data (Nadal and Bréon, 1999). Over land, Bréon et al. (2011) get a significant correlation (0.84) with the ground-based measurements. However, some discrepancy in the aerosol radius cutoff lead to an underestimation of the satellite retrieval compared to AERONET. In regions where dust-loaded atmospheres are excluded, i.e. in regions affected by biomass burning or pollution aerosols, particular comparisons with AERONET measurements show better results with no significant bias (Bréon et al., 2011; Tanré et al., 2011). A specific study (Fan et al., 2008) comparing AERONET data over Beijing and Xianghe in China demonstrated the capability of PARASOL for determining the anthropogenic contribution (particle radii less than or equal to 0.3 µm) of regional aerosols.

3 Validation results

During the year of 2005–2009, there are 124 and 149 PARASOL-AERONET AOD coincidences that met the data selection criteria for Beijing and Kanpur, respectively. At Beijing, less coincident counts (10) were obtained for spring, which is likely due to the eruption of dust storms during this season, leading to scant AERONET retrievals

AMTD
4, 5773–5806, 2011

within the accuracy criteria. During summer, there are only 4 and 7 coincidences for Beijing and Kanpur, respectively, which is mainly attributed to the large amount of precipitation at both sites. Summer is the rainy season and accounts for about 74 % and 88 % of the annual rainfall in Beijing and Kanpur, respectively (Yu et al., 2009; Eck et al., 2010), indicating severe cloud contamination that precludes aerosol observation. Table 1 lists the average statistic results of AOD (870 nm) comparison with collocated AERONET measurements for Beijing and Kanpur (relative difference and correlation coefficient). As PARASOL algorithm is sensitive to the accumulation mode of the aerosol size distribution, the comparisons statistic results of PARASOL AOD against fine mode AOD retrieved by AERONET (Dubovik and King, 2000; Dubovik et al., 2006) are also reported in Table 1. Validation against AERONET fine mode AOD shows an overall high correlation of $R^2 = 0.79$ for Beijing and $R^2 = 0.83$ for Kanpur. However, the PARASOL retrievals are found to underestimate aerosol optical depth by about 27 % and 34 % for Beijing and Kanpur, respectively. The AOD agreement is obviously poorer as compared to AERONET total AOD.

Table 1 demonstrates that AOD discrepancies with ground truth at both sites are obviously larger for spring and summer than for autumn and winter seasonsthis is largely related to the higher content of coarse dust particles during spring and summer seasons (Wang et al., 2011), resulting in stronger depolarization effect. At both sites, the retrieval error of PARASOL algorithm is found to be relatively higher for winter than that for autumn, which may arises from larger uncertainty in surface model for winter.

4 Discussion and analysis

4.1 Sensitive radius of polarized aerosol retrieval

Due to the scant PARASOL-AERONET AOD coincidences in summer (4 and 7 for Beijing and Kanpur, respectively), the analysis in this study focuses on the other three seasons.

AMTD
4, 5773–5806, 2011

Since only the accumulation mode of the aerosol size distribution can be retrieved from polarization measurements, we conduct study on the threshold radius of this fraction of size distribution, named as sensitive radius in this study. Considering that the fine-mode sensitive radius of polarized aerosol retrieval may depend on aerosol model, the investigation is conducted for different seasons at both Beijing and Kanpur.

First, seasonal mean refractive index and size distribution corresponding to the AOD coincidences are obtained from AERONET almucantar retrievals. The aerosol parameters are listed in Table 2. And Fig. 2 shows the seasonal averages of volume size distributions at Beijing (a) and Kanpur (b). Fan et al. (2008) found for the Beijing AERONET site a 0.3 µm particle radius threshold for fine-mode definition consistent with PARASOL retrievals, based on which a set of 30 fine mode cutoff radiuses are established between 0.19 µm and 0.43 µm with equal interval. For each fine mode cutoff radius, we use Mie codes to compute the corresponding fine-mode AOD at 670 and 870 nm, $\tau^{\lambda}_{\mathrm{fine\_}r}$, from seasonal mean refractive index and the fine-cutoff size distribution, assuming spherical scatterers which is valid for fine aerosols. The spectral polarized reflectance contributed by aerosols corresponding to each cutoff radius, $\rho^{\lambda}_{\mathrm{p\_}r}$, at the top of atmosphere (TOA), is simulated using RT3 vector radiative transfer model (Evans and Stephens, 1991), with a observation geometry of θ_{s}=52°, θ_{v}=40°, $\Delta\phi$=120°. This observation geometry is representative for PARASOL observation, moreover, in this geometry the scattering angle Θ is about 100°, corresponding to representative aerosol polarized phase function $q_{\mathrm{a}}(\Theta)$ (Deuzé et al, 2001), which can insure the generality of this analysis. Figures 3 and 5 show the computed seasonal spectral polarized reflectance

$\rho^{\lambda}_{\mathrm{p\_}r}$ for Beijing and Kanpur, respectively. Besides, the seasonal spectral polarized reflectance related to the entire size distribution (with particle radius ranging from 0 ~ 15 µm), $\rho^{\lambda}_{\mathrm{p\_15\,\mu m}}$, can be analogously estimated. To investigate the sensitivity of TOA polarized reflectance to fine-mode cutoff radius, we define the TOA polarized

AMTD
4, 5773–5806, 2011

reflectance difference between $\rho^{\lambda}_{\mathrm{p}\_r}$ and $\rho^{\lambda}_{\mathrm{p}\_15\,\mu m}$, $\Delta\rho_{\mathrm{p}\_r}$, for each cutoff radius as

$$\Delta\rho_{\mathrm{p}\_r} = \sqrt{(\rho^{870\,\mathrm{nm}}_{\mathrm{p}\_r} - \rho^{870\,\mathrm{nm}}_{\mathrm{p}\_15\,\mu m})^2 + (\rho^{670\,\mathrm{nm}}_{\mathrm{p}\_r} - \rho^{670\,\mathrm{nm}}_{\mathrm{p}\_15\,\mu m})^2} \tag{1}$$

4.1.1 Beijing

As shown in Fig. 3, at both 670 and 870 nm, the TOA polarized reflectance $\rho^{\lambda}_{\mathrm{p}\_r}$ for three seasons at Beijing exhibit similar variation tendency. With the increase of fine-mode cutoff radius r_{cutoff}, $\rho^{870\,\mathrm{nm}}_{\mathrm{p}\_r}$ firstly increases and then decreases with the peak value occurring at about 0.23 µm, while $\rho^{670\,\mathrm{nm}}_{\mathrm{p}\_r}$ decreases gradually. The variation ranges of $\rho^{870\,\mathrm{nm}}_{\mathrm{p}\_r}$ are much smaller than those of $\rho^{670\,\mathrm{nm}}_{\mathrm{p}\_r}$ (the maximum difference between maximum and minimum value at 870 nm is 0.13 %, while at 670 nm it can be up to 0.32 %). At both wavelengths, the TOA polarized reflectance is found to be highest during winter compared to those of spring and autumn seasons (see in Fig. 3). Winter also shows the largest variation range of $\rho^{870\,\mathrm{nm}}_{\mathrm{p}\_r}$ and $\rho^{670\,\mathrm{nm}}_{\mathrm{p}\_r}$ among all the seasons. This may arise from the higher volume fine mode concentration C_{fine} during winter (see Table 2). The TOA polarized reflectance of aerosols increases with the increase of C_{fine} since the measured polarized radiances are known to be mainly contributed by small particles. The fine-mode size distribution in spring is very close to that of autumn, as shown in Fig. 2a and Table 2. The slight difference of $\rho^{\lambda}_{\mathrm{p}\_r}$ between these two seasons (see in Fig. 3) can be attributed to the discrepancy in refractive index (see also Table 2).

Figure 4 illustrates the TOA polarized reflectance difference $\Delta\rho_{\mathrm{p}\_r}$ as a function of r_{cutoff} in three seasons at Beijing. It can be seen that $\Delta\rho_{\mathrm{p}\_r}$ of spring is significantly larger as compared to other seasons, which is primarily due to the higher volume coarse mode concentrations C_{coarse} during spring (see Table 2), resulting in stronger depolarization effect by large particles. Owing to the higher C_{fine} mentioned above, $\rho^{\lambda}_{\mathrm{p}\_r}$ of winter decreases sharply with the increase of r_{cutoff}. It should be noted that for all seasons,

AMTD
4, 5773–5806, 2011

X. F. Gu et al.

$\Delta\rho_{p\_r}$ reaches the minimum at r_{cutoff} of about 0.35 µm, after then $\Delta\rho_{p\_r}$ shows little change with the increase of r_{cutoff}.

4.1.2 Kanpur

Figure 5 shows that the seasonal and spectral variation trend of $\rho_{p\_r}^{870\,nm}$ and $\rho_{p\_r}^{670\,nm}$ at Kanpur is similar to that at Beijing. With the increase of fine-mode cutoff radius r_{cutoff}, $\rho_{p\_r}^{870\,nm}$ firstly increases and then decreases, while $\rho_{p\_r}^{670\,nm}$ decreases gradually. The variation ranges of $\rho_{p\_r}^{870\,nm}$ are much smaller than those of $\rho_{p\_r}^{670\,nm}$. At both wavelengths, the TOA polarized reflectance of post-monsoon and winter are found to be higher than that of pre-monsoon. This is primarily due to the lower seasonal mean C_{fine} and higher seasonal mean C_{coarse} in pre-monsoon season, as shown in Fig. 2b and Table 2. Unlike Beijing, the seasonal mean C_{fine} during pre-monsoon at Kanpur is significantly lower as compared to post-monsoon, as shown in Fig. 2b and Table 2. The fine-mode size distribution in post-monsoon has no evident difference compared with that of winter, however, $\rho_{p\_r}^{\lambda}$ of post-monsoon is found to be markedly higher, primarily due to the stronger scattering as well as weaker absorption by fine aerosols in post-monsoon (see the values of refractive index in Table 2). Similar analysis of the seasonal $\Delta\rho_{p\_r}$ as a function of r_{cutoff} at Kanpur is shown in Fig. 6. Higher $\Delta\rho_{p\_r}$ is found for pre-monsoon as compared to other seasons due to the depolarization by coarse aerosols, which is similar to Beijing. The difference in $\Delta\rho_{p\_r}$ between post-monsoon and winter can also be attributed to the higher C_{coarse} for post-monsoon season (see in Fig. 2b). From Fig. 6, similar results are also obtained for Kanpur that the minimum value of $\Delta\rho_{p\_r}$ appears at r_{cutoff} of about 0.35 µm, after then $\Delta\rho_{p\_r}$ do not change much with the increase of r_{cutoff}. So it comes to the conclusion that the fine-mode sensitivity radius for polarized aerosol retrieval is also about 0.35 µm. Such a value of 0.35 µm is also reported on the official website of PARASOL (http://smsc.cnes.fr/PARASOL/ae_prod.htm).

AMTD
4, 5773–5806, 2011

Table 3 presents the statistical results for comparison between PARASOL retrieved AOD and the AERONET AOD recomputed for radius <0.35 µm. The agreement is significantly improved, showing a correlation coefficient (R^2) of 0.82 with relative difference being 12 % for Beijing and 0.87 with relative difference being 19 % for Kanpur. The high correlation demonstrates remarkable sensitivity of PARASOL retrievals to the smaller fraction of fine particles with radius less than 0.35 µm. Table 3 shows that PAROSOL aerosol retrieval algorithm performs best for autumn. For spring and summer seasons, relatively larger discrepancies still appear.

The analysis indicates that some discrepancy between the sensitive radius of PARASOL and the fine mode separation radius of AERONET is an important influencing factor for validation of PARASOL algorithm.

4.2 Sensitivity of the retrieved AOD to aerosol properties

The measured polarized light at TOA consists of contributions from molecules, aerosols and the underlying surface, which can be expressed as (Deuzé et al., 2001)

$$Q_{\text{meas}} = Q_{\text{m}} + e^{-M\tau_{\text{m}}}\left(\frac{\tau_{\text{a}}q_{\text{a}}}{4\cos\theta_v} + e^{-M\beta\tau_{\text{a}}}R_{\text{p}}^{\text{g}}\right) \quad (2)$$

where Q_{m} is the molecular contribution, τ_{m} and τ_{a} are the molecular and aerosol optical depth, respectively, q_{a} is the aerosol polarized phase function and

R_{p}^{g} is the surface polarized reflectance, θ_{v} is the viewing zenith angle, and M is the air mass factor. Here β accounts for the large forward scattering of the aerosols with a value of about 0.50. To facilitate analysis on the impact of the assumed refractive index and size distribution to PARASOL aerosol retrieval, we ignore the uncertainty on the molecular contribution, which is considered to be valid in channels centered at 670 and 865 nm. Concerning the accumulation mode, a set of ten modal effective radii ranging from 0.075 to 0.225 µm with standard deviation $\sigma = 0.403$, and a refractive index m = 1.47–0.01i are assumed in PARASOL standard aerosol retrieval algorithm. The uncertainty in the calculated aerosol polarized phase function $q_{\text{a}}^{\text{cal}}$ arising from this

AMTD
4, 5773–5806, 2011

assumption would lead to uncertainty in the derived τ_a, which can be approximately expressed as

$$Q_{cal} = \frac{\tau_m q_m}{4\cos\theta_v} + e^{-M\tau_m}\left(\frac{\tau_a(1+\eta_{\tau_t}^{q_a})q_a^{cal}}{4\cos\theta_v} + e^{-M\beta\tau_a(1+\eta_{\tau_t}^{q_a})}R_p^g\right) \tag{3}$$

where $\eta_{\tau_t}^{q_a}$ is the error of the retrieved AOD against AEROENT total AOD arising from q_a^{cal}.

From Eq. (2), given different surface polarized reflectances R_p^g, the same uncertainty in $q_a(\Theta)$ may result in different retrieval errors of τ_a. According to Nadal and Bréon (1999), the land surface polarized reflectance generally varies in the range of 0–3 %. So we investigate the impact of refractive index and size distribution to τ_a for 4 values of R_p^g, i.e. 0.5%, 1%, 2%, 3%.

The seasonal mean refractive index and size distribution obtained from are used to calculate the true value of q_a and τ_a in Eq. (2) using Mie theory. While q_a^{cal} is estimated from the refractive index of m = 1.47–0.01i and the fine mode fraction of the seasonal mean size distribution, which is assumed to roughly agree with the size distribution used in PARASOL retrieval. The seasonal mean Angstrom exponent $\alpha_{670-865\,nm}$ derived by PARASOL and those estimated from the fine-mode size distribution of AERONET with m = 1.47–0.01i are given in Table 4. It can be seen that the relative differences between two independently derived α are generally under 10 % at both sites, indicating the reliability of this assumption. Nevertheless, relatively larger discrepancy appears for winter at Kanpur.

For each surface polarized reflectance R_p^g, discrete values of $\eta_{\tau_t}^{q_a}$ between −100 % and 200 % (intervals of 5 %) are preset. The solution is the one where Q_{cal} best matches Q_{meas}, i.e. the one corresponds to the minimum absolute value of difference ΔQ:

$$\Delta Q = e^{-M\tau_m}\left[\frac{\tau_a(1+\eta_{\tau_t}^{q_a})q_a^{cal}}{4\cos\theta_v} + e^{-M\beta\tau_a(1+\eta_{\tau_t}^{q_a})}R_p^g - \left(\frac{\tau_a q_a}{4\cos\theta_v} + e^{-M\beta\tau_a}R_p^g\right)\right] \tag{4}$$

AMTD
4, 5773–5806, 2011

The estimation is performed in similar observation geometry of $\theta_s = 40^\circ$, $\theta_v = 40^\circ$ for a set of scattering angle Θ ranging from 0–180°.

The retrieval errors against AERONET AOD recomputed for radius <0.35 µm arising from q_a^{cal}, expressed as

$\eta_{\tau_s}^{q_a}$, can be analogously estimated. The difference is that aerosol optical depth and aerosol phase function are simulated for radius <0.35 µm.

As aerosols exhibit probably negative or positive (parallel to the scattering plane) in angular range near $\Theta = 180^\circ$ and $\Theta = 0^\circ$ (see in Fig. 2 in Deuzé et al., 2001), we focus on the polarized light scattered in the range $30^\circ < \Theta < 130^\circ$ where polarization is relatively large, and the angular average errors are considered to give a general assessment. The two kinds of errors are listed in Tables 5 and 6, respectively.

At both Beijing and Kanpur, the retrieval errors caused by uncertainty in $q_a(\Theta)$ are found to be higher in spring than those of autumn and winter seasons. For higher surface polarized reflectance, the error $\eta_{\tau_t}^{q_a}$ can even reach −100 %. This is primarily attributed to the strong impact of the long-range advected desert dust during spring (Eck et al., 2010), resulting in much smaller $q_a(\Theta)$ than that of the PARASOL algorithm which accounts for the underestimate of PARASOL retrieved AOD. As listed in Tables 5 and 6, the errors caused by q_a^{cal} for spring are found to be larger at Kanpur compared to Beijing, due to the higher volume coarse mode concentrations C_{coarse} at Kanpur (see Table 2). Table 3 also illustrates that $\eta_{\tau_t}^{q_a}$ decreases in autumn and winter seasons with the minimum occurs in winter. At Beijing, the lower $\eta_{\tau_t}^{q_a}$ of winter possibly result from its higher C_{fine} as compared to autumn, given similar C_{coarse} for two seasons. While at Kanpur, the reason contrarily lies in the lower C_{coarse} during winter given similar C_{fine}. Both causes lead to smaller uncertainty in $q_a(\Theta)$.

It can be seen from Tables 5 and 6 that $\eta_{\tau_s}^{q_a}$ are significantly lower than $\eta_{\tau_t}^{q_a}$, with similarly larger errors in spring. Table 5, together with Table 1, reveal that errors contributed by uncertainty in $q_a(\Theta)$ is much close to the total errors listed in Table 1 (accounts for about 65 % to 94 %, except for spring at Kanpur which is specially discussed in Sect. 4.3), which indicates that the overestimate of $q_a(\Theta)$ in PARASOL algorithm

AMTD
4, 5773–5806, 2011

contributes mostly to the underestimate of retrieved AOD.

4.3 Uncertainty of surface model for polarized reflectance

The differences between errors of τ_a introduced by uncertainty in $q_a(\Theta)$ (see Table 5) and the total errors (see Table 1) come from the uncertainty of surface model. Considering the influence of surface model, Eq. (3) can be rewritten as

$$Q_{\mathrm{cal}} = \frac{\tau_m q_m}{4\cos\theta_v} + e^{-M\tau_m}\left(\frac{\tau_a(1+\eta_{\tau_t})q_a^{\mathrm{cal}}}{4\cos\theta_v} + e^{-M\beta\tau_a(1+\eta_{\tau_t})}R_p^{\mathrm{cal}}\right) \tag{5}$$

where η_{τ_t} is the total errors of τ_a (listed in Table 1), and R_p^{cal} is the modeled surface polarized reflectance used in PARASOL retrieval. Here we estimate R_p^{cal} from the equality of Eqs. (2) and (5) for each of the four values of R_p^{g} which are considered as true values, finally the uncertainty of surface BPDF model can be obtained and are listed in Table 7. Here the estimation is performed in the same observation geometry with those in Sect. 4.2.

Except for spring at Kanpur, surface polarization is overestimated in various levels for different surface polarized reflectances. The average uncertainties (about 20 %–50 %) show good agreement with previous study (Waquet et al., 2007), which reported that the surface model overestimates surface polarization from a few to fifty percents.

At both sites, the surface model demonstrates the poorest performance for winter season, which can be attributed to low vegetation coverage during winter leading to higher polarization than predicted in the model. Ice and snow cover may even appear during winter at Beijing. The even higher uncertainty for winter at Kanpur possibly results from the impact of the size distribution assumption, as mentioned above, the discrepancy between two independently derived α is relatively larger($\sim$13.1 %) for winter at Kanpur (see Table 4).

The unusual underestimate of the modeled polarized reflectance, in spring at Kanpur, probably arises from the inadequacy of Mie calculations of $q_a(\Theta)$ for the coarse-dominated particles which might be nonspherical (Mishchenko and Travis, 1998).

AMTD
4, 5773–5806, 2011

5 Conclusions

Sensitivity study on the PARASOL aerosol retrieval algorithm over land is presented for aerosol mixtures composed of fine mode pollution particles combined with coarse mode desert dust. First an assessment of the PARASOL aerosol products during the period of 2005–2009 is investigated by comparison with both the total AOD and fine mode AOD derived by AERONET at Beijing and Kanpur.

Validation against AERONET fine mode AOD shows an overall high correlation of $R^2 = 0.79$ for Beijing and $R^2 = 0.83$ for Kanpur. However, the PARASOL retrievals are found to underestimate aerosol optical depth by about 27 % and 34 % for Beijing and Kanpur, respectively. The AOD agreement is obviously poorer as compared to AERONET total AOD. The results show that, at both sites, the PARASOL polarization retrieval algorithm performs better in autumn and winter seasons, which is largely related to the higher content of coarse dust particles during spring and summer seasons. For winter, the AOD agreement is obviously poorer as compared to autumn, which may arises from larger uncertainty in surface polarized reflectance model because of the low vegetation coverage during winter.

Due to the scant PARASOL-AERONET AOD coincidences in summer (4 and 7 for Beijing and Kanpur, respectively), the analysis in this study focuses on the other three seasons. As PARASOL aerosol algorithm is sensitive to the accumulation mode of the aerosol size distribution, we conduct study on the sensitive radius of polarized aerosol retrieval for different seasons at both Beijing and Kanpur. The results show that the sensitive radius for PARASOL retrievals is 0.35 µm for all seasons. And the agreement is significantly improved by employing comparison against the AERONET AOD recomputed for radius <0.35 µm, showing a correlation coefficient (R^2) of 0.82 with relative difference being 12 % for Beijing and 0.87 with relative difference being 19 % for Kanpur.

The impact of assumed refractive index and size distribution to the retrieved AOD is investigate for 4 values of surface polarized reflectance, i.e. 0.5 %, 1 %, 2 %, 3 %.

AMTD
4, 5773–5806, 2011

The seasonal mean refractive index and size distribution obtained from AERONET inversions are used to calculate the true aerosol polarized phase function $q_a(\Theta)$ using Mie theory. While the aerosol polarized phase function q_a^{cal} used in PARASOL retrieval is estimated from the refractive index of m = 1.47–0.01i and the fine mode fraction of the seasonal mean size distribution, which is assumed to roughly agree with the size distribution of PARASOL retrieval. Comparison between the Angstrom exponent $\alpha_{670-865\,\mathrm{nm}}$ derived by PARASOL and that estimated from the fine-mode size distribution of AERONET with m = 1.47–0.01i indicates the reliability of this assumption.

The sensitivity study on uncertainty of PARASOL aerosol retrieval demonstrates that the overestimate of $q_a(\Theta)$ in PARASOL algorithm contributes mostly to the underestimate of retrieved AOD (accounts for about 65 % to 94 % in different seasons). Uncertainties caused by q_a^{cal} are significantly higher in spring than those of autumn and winter seasons. This is largely related to the strong impact of the long-range advected desert dust during the spring season in both regions, resulting in much lower aerosol-polarized phase function $q_a(\Theta)$ compared to the PARASOL algorithm. The aerosol retrieval errors caused by q_a^{cal} for spring are found to be higher at Kanpur, due to the obviously higher content of coarse dust particles compared to Beijing.

Investigation on the uncertainty of the surface contribution shows that the Nadal and Bréon BPDF surface model overestimates surface polarization from about 20 % to 50 % percents with the maximum uncertainties occurring in winter, which can be possibly attributed to low vegetation coverage during winter leading to higher polarization than predicted in the model. The unusual underestimate of the surface polarization, in spring at Kanpur, probably arises from the inadequacy of Mie calculations of $q_a(\Theta)$ for the coarse-dominated particles which might be nonspherical.

Acknowledgements. This work was supported by the National Basic Research Program of China (973 Program) (Grant No: 2010CB950800), the International Science and Technology Cooperation Program of China (2010DFA21880), and the Bilateral Inter- Governmental Science and Technology Cooperation Program ([2008]333). We thank the PIs H. B. Chen and P. Goloub and B. N. Holben and R. P. Singh for their effort in establishing and maintaining the Beijing and

AMTD

4, 5773–5806, 2011

PARASOL in Beijing and Kanpur

X. F. Gu et al.

Kanpur AERONET sites used in this investigation. We are also thankful to the ICARE center for providing the PARASOL level 1 and level 2 data we used in this study.

References

Bréon, F. M., Vermeulen, A., and Descloitres, J.: An evaluation of satellite aerosol products against sunphotometer measurements, Remote Sens. Environ., doi:10.1016/j.rse.2011.06.017, 2011.

Charlson, R. J., Schwartz, S. E., Hales, J. M., Cess, R. D., Coakley Jr., J. A., Hansen, J. E., and Hofmann, D. J.: Climate Forcing by Anthropogenic Aerosols, Science, 255, 504324, 423–430, 1992.

Deschamps, P. Y., Bréon, F. M., Leroy, M., Podaire, A., Bricaud, A., Buriez, J. C., and Seze, G.: The POLDER mission: Instrument characteristics and scientific objectives, IEEE T. Geosci. Remote Sens., 32, 598–615, 1994.

Deuzé, J. L., Bréon, F. M., Devaux, C., Goloub, P., Herman, M., Lafrance, B., Maignan, F., Marchand, A., Nadal, F., Perry, G., and Tanré, D.: Remote sensing of aerosols over land surfaces from POLDER-ADEOS-1 polarized measurements, J. Geophys. Res., 106, 4913–4926, 2001.

Dubovik, O.: Optimization of numerical inversion in photopolarimetric remote sensing, in: Photopolarimetry in Remote Sensing, edited by: Videen, G., Yatskiv, Y., and Mishchenko, M., Kluwer Academic Publishers, Dordrecht, The Netherlands, 65–106, 2004.

Dubovik, O. and King, M. D.: A flexible inversion algorithm for retrieval of aerosol optical properties from Sun and sky radiance measurements, J. Geophys. Res., 105, 20673–20696, 2000.

Dubovik, O., Sinyuk, A., Lapyonok, T., Holben, B. N., Mishchenko, M., Yang, P., Eck, T. F., Volten, H., Munoz, O., Veihelmann, B., van der Zander, W. J., Leon, J.-F., Sorokin, M., and Slutsker, I.: Application of light scattering by spheroids for accounting for particle non-sphericity in remote sensing of desert dust, J. Geophys. Res., 111, D11208, doi:10.1029/2005JD006619, 2006.

Dubovik, O., Herman, M., Holdak, A., Lapyonok, T., Tanré, D., Deuzé, J. L., Ducos, F., Sinyuk, A., and Lopatin, A.: Statistically optimized inversion algorithm for enhanced retrieval of

AMTD
4, 5773–5806, 2011

PARASOL in Beijing and Kanpur

X. F. Gu et al.

aerosol properties from spectral multi-angle polarimetric satellite observations, Atmos. Meas. Tech., 4, 975—1018, doi:10.5194/amt-4-975-2011, 2011.

Eck, T. F., Holben, B. N., Sinyuk, A., Pinker, R. T., Goloub, P., Chen, H., Chatenet, B., Li, Z., Singh, R. P., Tripathi, S. N., Reid, J. S., Giles, D. M., Dubovik, O., O'Neill, N. T., Smirnov, A., Wang, P., and Xia, X.: Climatological aspects of the optical properties of fine/coarse mode aerosol mixtures, J. Geophys. Res., 115, D19205, doi:10.1029/2010JD014002, 2010.

Evans, K. F. and Stephens, G. L.: A new polarized atmospheric radiative transfer model, J. Quant. Spec. Ra., 46, 413–423, 1991.

Fan, X. H., Goloub, P., Deuzé, J. L., Chen, H. B., Zhang, W. X., Tanré, D., and Li, Z. Q.: Evaluation of PARASOL aerosol retrieval over North East Asia, Remote Sens. Environ., 112, 697–707, 2008.

Hansen, J., Sato, M., and Ruedy, R.: Radiative forcing and climate response, J. Geophys. Res., 102, 6831–6864, 1997.

Hansen, J., Nazarenko, L., Ruedy, R., Sato, M., Willis, J., Del Genio, A., Koch, D., Lacis, A., Lo, K., Menon, S., Novakov, T., Perlwitz, J., Russell, G., Schmidt, G. A., and Tausnev, N.: Earth's energy imbalance: Confirmation and implications, Science, 308, 1431–1435, 2005.

Herman, M., Deuzé, J. L., Devaux, C., Goloub, P., Bréon, F. M., and Tanré, D.: Remote Sensing of Aerosols over Land Surfaces Including Polarization Measurements: Applications to POLDER Measurements, J. Geophys. Res., 102, 17039–17050, 1997.

Holben, N., Eck, T. F., Slutsker, I., Tanré, D., Buis, J. P., Setzer, A.,Vermote, E., Reagan, J. A., Kaufman, Y. J., Nakajima, T., Lavenu, F., Jankowiak, I., and Smirnov, A.: AERONET – A federated instrument network and data archive for aerosol characterization, Remote Sens. Environ., 66, 1–16, 1998.

Holben, B. N., Tanré, D., Smirnov, A., Eck, T. F., Slutsker, I., Abuhassan, N., Newcomb, W. W., Schafer, J. S., Chatenet, B., Lavenu, F., Kaufman, Y. J., Vande Castle, J., Setzer, A., Markham, B., Clark, D., Frouin, R., Halthore, R., Karneli, A., O'Neill, N. T., Pietras, C., Pinker, R. T., Voss, K., and Zibordi, G.: An emerging ground?based aerosol climatology: Aerosol optical depth from AERONET, J. Geophys. Res., 106, 12067–12097, doi:10.1029/2001JD900014, 2001.

Kahn, R. A., Gaitley, B. J., Garay, M. J., Diner, D. J., Eck, T. F., Smirnov, A., and Holben, B. N.: Multiangle Imaging SpectroRadiometer global aerosol product assessment by comparison with the Aerosol Robotic Network, J. Geophys. Res., 115, D23209, doi:10.1029/2010JD014601, 2010.

Kaufman, Y. J., Tanré, D., Remer, L., Vermote, E., Chu, A., and Holben, B.: Operational remote sensing of tropospheric aerosol over land from EOS moderate resolution imaging spectroradiometer, J. Geophys. Res., 102, 17051–17067, 1997.

Kokhanovsky, A. A. and de Leeu, G. W.: Satellite Aerosol Remote Sensing Over Land, Praxis Publishing Ltd, Chichester, UK, 2009.

Kokhanovsky, A. A., Deuzé, J. L., Diner, D. J., Dubovik, O., Ducos, F., Emde, C., Garay, M. J., Grainger, R. G., Heckel, A., Herman, M., Katsev, I. L., Keller, J., Levy, R., North, P. R. J., Prikhach, A. S., Rozanov, V. V., Sayer, A. M., Ota, Y., Tanré, D., Thomas, G. E., and Zege, E. P.: The inter-comparison of major satellite aerosol retrieval algorithms using simulated intensity and polarization characteristics of reflected light, Atmos. Meas. Tech., 3, 909–932, doi:10.5194/amt-3-909-2010, 2010.

Levy, R. C., Remer, L. A., Mattoo, S., Vermote, E. F., and Kaufman, Y. J.: Second-generation operational algorithm: Retrieval of aerosol properties over land from inversion of Moderate Resolution Imaging Spectroradiometer spectral reflectance, J. Geophys. Res., 112, D13211, doi:10.1029/2006JD007811, 2007.

Martonchik, J. V., Diner, D. J., Kahn, R., Verstraete, M. M., Pinty, B., Gordon, H. R., and Ackerman, T. P.: Techniques for the Retrieval of aerosol properties over land ocean using multiangle data, IEEE T. Geosci. Remote Sens., 36, 1212–1227, 1998.

Mishchenko, M. I. and Larry, D. Travis: Capabilities and limitations of a current FORTRAN implementation of the T-matrix method for randomly oriented, rotationally symmetric scatterers, J. Quant. Spec. Ra., 60, 309–324, 1998.

Mishchenko, M. I., Cairns, B., Kopp, G., Schueler, C. F., Fafaul, B. A., Hansen, J. E., Hooker, R. J., Itchkawich, T., Maring, H. B., and Travis, L. D.: "Accurate monitoring of terrestrial aerosols and total solar irradiance: introducing the Glory mission," B. Am. Meteorol. Soc., 88, 677–691, doi:10.1175/BAMS-88-5-677, 2007.

Nadal, F. and Bréon, F. M.: Parameterization of surface polarized reflectance derived from POLDER spaceborne measurements, IEEE T. Geosci. Remote Sens., 37, 1709–1718, 1999.

Nemesure, S., Wagener, R., and Schwartz, S.: Direct shortwave forcing of climate by the anthropogenic sulfate aerosol: Sensitivity to particle size, composition, and relative humidity, J. Geophys. Res., 100, 26105–26116, 1995.

Ramanathan, V., Crutzen, P., Kiehl, J., and Rosenfeld, D.: Aerosols, Climate, and the Hydrological Cycle, Science, 294, 2119–2124, 2001.

AMTD

4, 5773–5806, 2011

PARASOL in Beijing and Kanpur

X. F. Gu et al.

Smirnov, A., Holben, B. N., Eck, T. F., Dubovik, O., and Slutsker, I.: Cloud screening and quality control algorithms for the AERONET database, Remote Sens. Environ., 73, 337–349, 2000.
Singh, R. P., Dey, S., Tripath, S. N. I, Tare, V., and Holben, B.: Variability of aerosol parameters over Kanpur, northern India, J. Geophys. Res., 109, D23206, doi:10.1029/2004JD004966, 2004.
Tanré D.: Derivation of tropospheric aerosol properties from satellite observations, C. R. Geoscience, 342, 403–411, 2010.
Tanré, D., Bréon, F. M., Deuzé, J. L., Dubovik, O., Ducos, F., Francois, P., Goloub, P., Herman, M., Lifermann, A., and Waquet, F.: Remote sensing of aerosols by using polarized, directional and spectral measurements within the A-Train: the PARASOL mission, Atmos. Meas. Tech., 4, 1383–1395, doi:10.5194/amt-4-1383-2011, 2011.
Wang, S., Fang, L., Gu, X., Yu, T., and Gao, J.: Comparison of aerosol optical properties from Beijing and Kanpur, in press, Atmos. Environ., doi:10.1016/j.atmosenv.2011.06.055, 2011.
Waquet, F., Goloub, P., Deuzé, J.-L., Léon, J. F., Auriol, F., Verwaerde, C., Balois, J. Y., François, P.: Aerosol Retrieval Over Land using a multiband polarimeter and comparison with path radiance method, J. Geophys. Res., 112, D11214, doi:10.1029/2006JD008029, 2007.
Yu, X., Zhu, B., and Zhang, M.: Seasonal variability of aerosol optical properties over Beijing, Atmos. Environ., 43, 4095–4101, 2009.

AMTD
4, 5773–5806, 2011

Table 1. Average statistics for PARASOL-AERONET AOD comparison at Beijing and Kanpur*.

	Beijing					Kanpur				
Season/	N	Against τ_{AER}^{total}		Against τ_{AER}^{fine}		N	Against τ_{AER}^{total}		Against τ_{AER}^{fine}	
Total		Rel. Diff.	R^2	Rel. Diff.	R^2		Rel. Diff.	R^2	Rel. Diff.	R^2
Spring	10	−78 %	0.74	−50 %	0.90	54	−84 %	0.31	−37 %	0.64
Summer	4	−86 %	0.88	−63 %	0.91	7	−90 %	0.59	−44 %	0.47
Autumn	62	−55 %	0.61	−10 %	0.81	49	−50 %	0.66	−22 %	0.86
Winter	48	−63 %	0.87	−37 %	0.86	36	−57 %	0.75	−43 %	0.82
Total	**124**	**−60 %**	**0.71**	**−27 %**	**0.79**	**146**	**−67 %**	**0.17**	**−34 %**	**0.83**

* N: Counts of coincidences; τ_{AER}^{total}: AERONET total AOD; τ_{AER}^{fine}: AERONET fine mode AOD; Rel. Diff.: relative difference; R^2: correlation coefficient.

AMTD
4, 5773–5806, 2011

Table 2. Seasonal mean aerosol physical parameters from AERONET almucantar retrievals corresponding to the AOD coincidences.

Season	Beijing			Kanpur		
	m	C_{fine}	C_{coarse}	m	C_{fine}	C_{coarse}
Spring	1.586–0.012i	0.044	0.148	1.533–0.010i	0.042	0.265
Summer	1.578–0.012i	0.025	0.084	1.490–0.007i	0.040	0.514
Autumn	1.554–0.018i	0.049	0.092	1.543–0.013i	0.078	0.132
Winter	1.568–0.019i	0.069	0.088	1.533–0.022i	0.079	0.087

Table 3. Average statistics for comparison of PARASOL AOD against AERONET AOD recomputed for $r < 0.35\,\mu m$ at Beijing and Kanpur*.

Season	Beijing		Kanpur	
	Rel. Diff.	R^2	Rel. Diff.	R^2
Spring	−44 %	0.89	−22 %	0.63
Summer	−59 %	0.92	−25 %	0.34
Autumn	−3 %	0.82	−9 %	0.87
Winter	−24 %	0.90	−28 %	0.87
Total	**−12 %**	**0.82**	**−19 %**	**0.87**

AMTD
4, 5773–5806, 2011

Table 4. Seasonal mean $\alpha_{670-865\,\mathrm{nm}}$ retrieved by PARASOL and those estimated from AERONET fine-mode size distribution.

Season	Beijing			Kanpur		
	α_{PAR}	α_{AER}	Rel. Diff.	α_{PAR}	α_{AER}	Rel. Diff.
Spring	2.42	2.36	2.6 %	2.43	2.63	8 %
Autumn	2.23	1.99	10.7 %	2.21	2.14	3.2 %
Winter	2.22	2.06	7.2 %	2.26	1.97	13.1 %

AMTD
4, 5773–5806, 2011

Table 5. Retrieval errors against AEROENT total AOD introduced by the uncertainty in $q_a(\Theta)$.

R_p^g	Beijing			Kanpur		
	Spring	Autumn	Winter	Premonsoon	Postmonsoon	Winter
$R_p^g = 0.005$	−67 %	−43 %	−39 %	−93 %	−42 %	−31 %
$R_p^g = 0.01$	−69 %	−44 %	−41 %	−94 %	−43 %	−34 %
$R_p^g = 0.02$	−75 %	−51 %	−47 %	−98 %	−49 %	−39 %
$R_p^g = 0.03$	−80 %	−58 %	−54 %	−100 %	−55 %	−44 %
Average	**−73 %**	**−49 %**	**−45 %**	**−96 %**	**−47 %**	**−37 %**

AMTD
4, 5773–5806, 2011

Table 6. Retrieval errors against AEROENT recomputed AOD for $r < 0.35\,\mu m$ introduced by the uncertainty in $q_a(\Theta)$.

R_p^g	Beijing			Kanpur		
	Spring	Autumn	Winter	Premonsoon	Postmonsoon	Winter
$R_p^g = 0.005$	−21 %	19 %	13 %	−63 %	5 %	16 %
$R_p^g = 0.01$	−25 %	15 %	10 %	−72 %	2 %	13 %
$R_p^g = 0.02$	−40 %	2 %	−2 %	−91 %	−8 %	3 %
$R_p^g = 0.03$	−52 %	−13 %	−14 %	−100 %	−19 %	−6 %
Average	**−35 %**	**6 %**	**2 %**	**−82 %**	**−5 %**	**6 %**

Discussion Paper | Discussion Paper | Discussion Paper | Discussion Paper |

AMTD

4, 5773–5806, 2011

PARASOL in Beijing and Kanpur

X. F. Gu et al.

AMTD
4, 5773–5806, 2011

PARASOL in Beijing and Kanpur

X. F. Gu et al.

Table 7. Uncertainties of surface model for different surface polarized reflectances.

R_p^g	Beijing			Kanpur		
	Spring	Autumn	Winter	Premonsoon	Postmonsoon	Winter
$R_p^g = 0.005$	57 %	44 %	107 %	−77 %	56 %	130 %
$R_p^g = 0.01$	24 %	19 %	49 %	−45 %	25 %	59 %
$R_p^g = 0.02$	5 %	5 %	18 %	−30 %	7 %	25 %
$R_p^g = 0.03$	0 %	1 %	9 %	−22 %	1 %	13 %
Average	**22 %**	**17 %**	**46 %**	**−44 %**	**22 %**	**57 %**

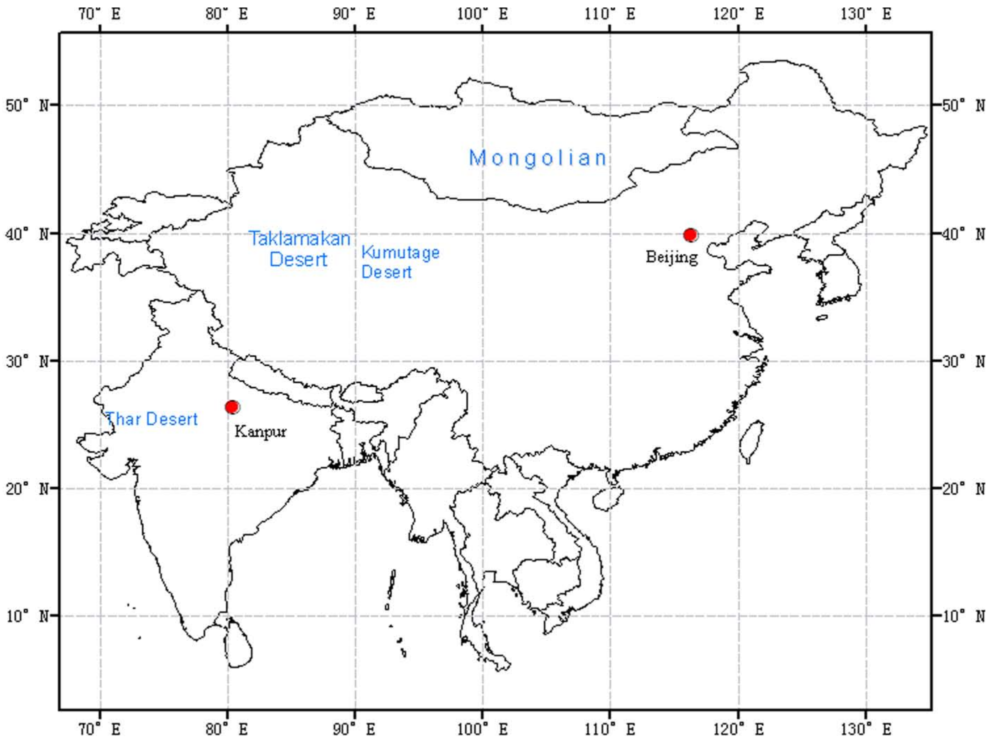

Fig. 1. Map showing the location of Beijing and Kanpur AERONET sites.

AMTD
4, 5773–5806, 2011

PARASOL in Beijing and Kanpur

X. F. Gu et al.

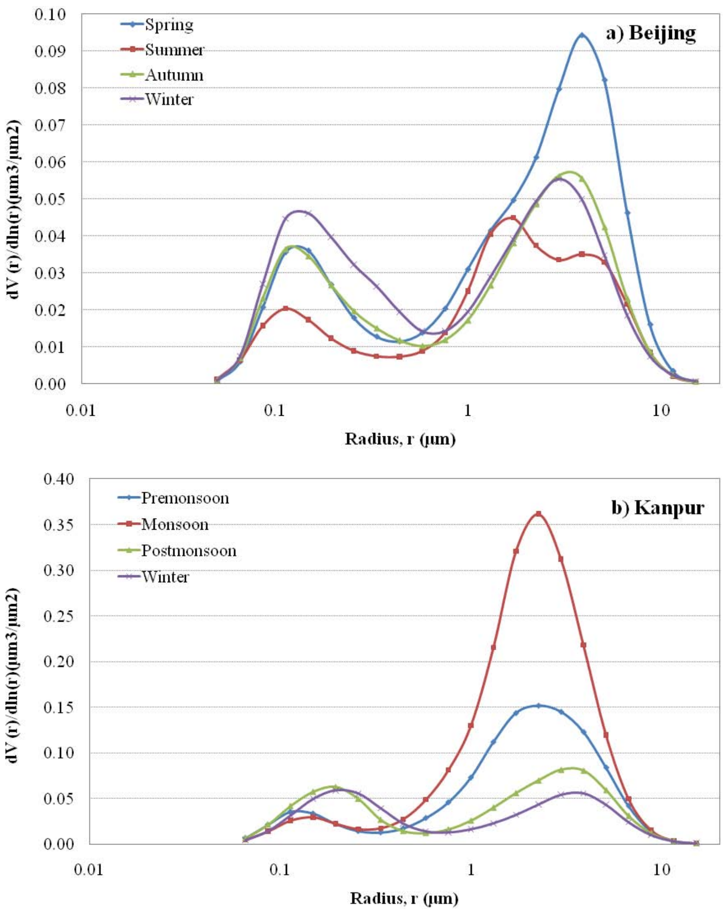

Fig. 2. Seasonal average aerosol volume size distributions corresponding to the AOD coincidences derived from AERONET retrievals for **(a)** Beijing and **(b)** Kanpur.

AMTD
4, 5773–5806, 2011

PARASOL in Beijing and Kanpur

X. F. Gu et al.

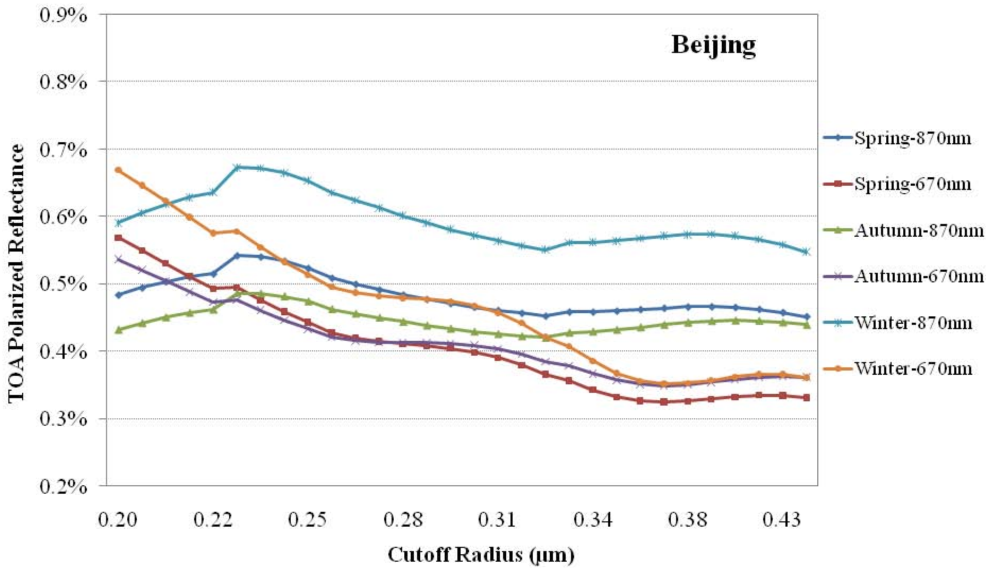

Fig. 3. The simulated seasonal spectral polarized reflectance at TOA for Beijing.

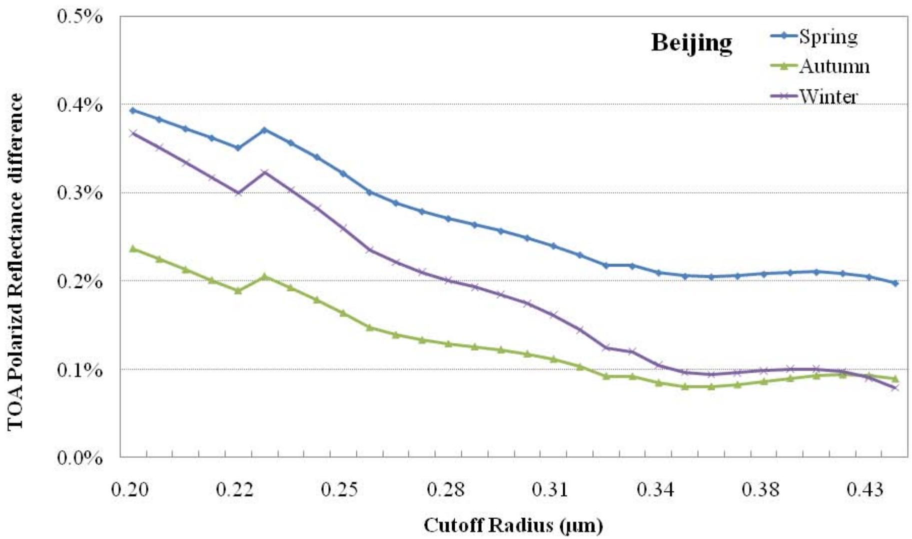

Fig. 4. The seasonal polarized reflectance difference at TOA for Beijing.

Discussion Paper | Discussion Paper | Discussion Paper | Discussion Paper

AMTD

4, 5773–5806, 2011

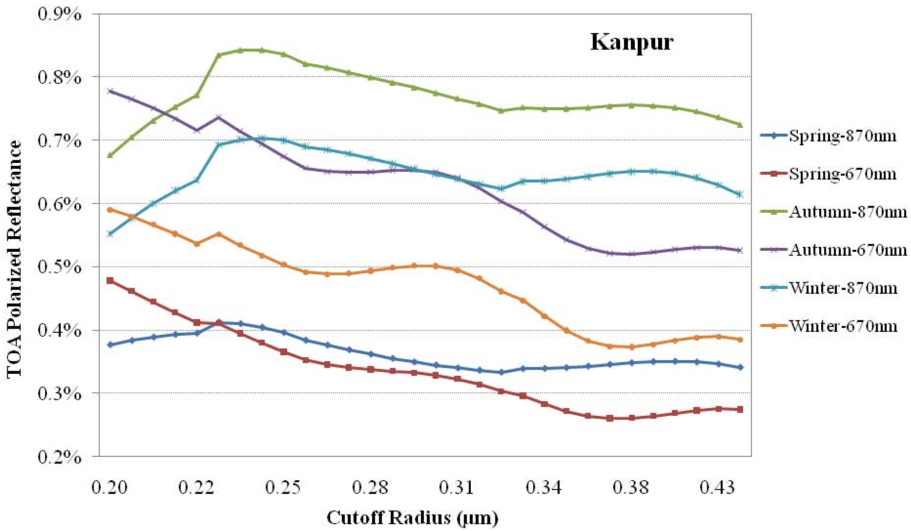

Fig. 5. The simulated seasonal spectral polarized reflectance at TOA for Kanpur.

AMTD
4, 5773–5806, 2011

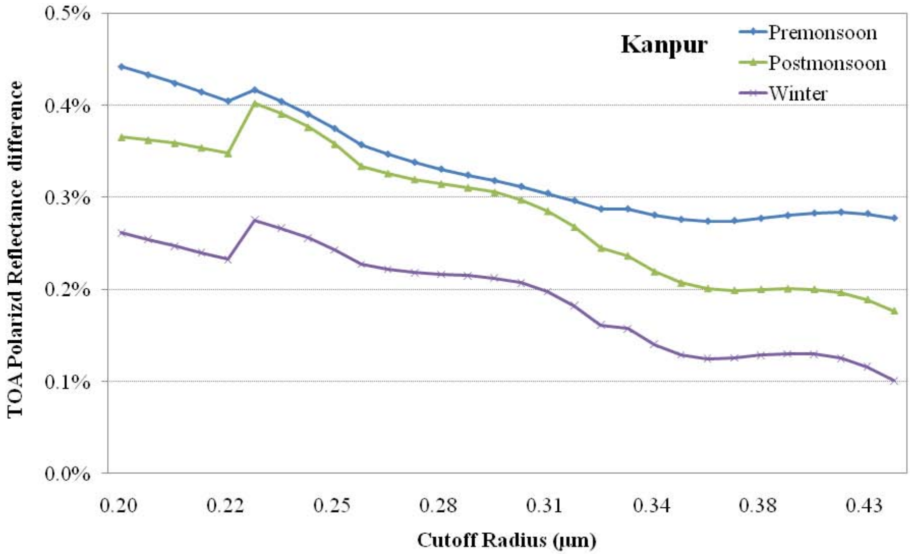

Fig. 6. The seasonal polarized reflectance difference at TOA for Kanpur.

AMTD
4, 5773–5806, 2011

PARASOL in Beijing and Kanpur

X. F. Gu et al.

Title Page
Abstract Introduction
Conclusions References
Tables Figures
◀ ▶
Back Close
Full Screen / Esc
Printer-friendly Version
Interactive Discussion